I. Yazar*

Simulation of a High Fidelity Turboshaft Engine-Alternator Model for Turboelectric Propulsion System Design and Applications

https://doi.org/10.1515/tjj-2018-0036
Received October 14, 2018; accepted October 22, 2018

Abstract: The term sustainability became a popular subject both in the automotive industries and in the aerospace industries. Increasing and threatening environmental pollution problems and reduction in limited fuel sources are motivating either industries and academicians to develop alternative power systems to sustain more healthier and economical life in the long term. One innovation that has been researched in the automotive industry is all electric and hybrid electric propulsion concepts. These concepts have also been proposed as alternative solutions for aviation. These novel propulsion technologies are composed of a gas turbine/internal combustion engine structure (necessary for hybrid electric and turboelectric propulsion systems) and/or energy storage components (battery, fuel cell and so on.) with multiple electric motors respectively. In this paper, simulation of a high fidelity turboshaft engine-alternator model for turboelectric propulsion system is derived. To develop an aero-thermal engine model, GE T700 turboshaft engine data is used and constructed model is connected to an alternator model on MATLAB/Simulink environment. Open-loop simulations are carried out and satisfactory results are obtained.Simulation results are compared to the real engine design point data. Results show that there are acceptable differences between the simulation results and the real engine data. The power balances between compressor - high pressure turbine and power turbine – alternator are proven in the mathematical model. It is expected that the proposed model can be easily extended to power system design and power management studies in turboelectric propulsion systems and also in other suitable novel propulsion systems.

***Corresponding author: I. Yazar,** Department of Mechatronics, Eskisehir Osmangazi Univesity, Eskisehir Vocational School, Industrial Zone Campus, Eskisehir, 26110, Turkey,
E-mail: iyazar@ogu.edu.tr

Keywords: turboshaft engine aero-thermal model, alternator, turboelectric propulsion system

PACS 2010 Classification: 05.70.Ce Thermodynamic functions and equations of state, 07.05.Tp Computer modeling and simulation, 89.40.Dd Air transporation, 88.05.Xj Energy use in transportation, 88.85.Hj Electric vehicles (EVs), 88.85.Fg Plug-in hybrid vehicles (HEVs)

Introduction

Today's propulsion technology still uses fossil fuels and they have a negative impact on the environment [1]. In addition to this, limited fuel reserves point at the requirement of alternative propulsion solutions. Novel propulsion technologies to aircraft of any size, generally named as electric propulsion, hybrid electric propulsion and turboelectric, are seen as viable and clean solutions for aviation [2]. These new type of propulsion technologies are aimed to reduce carbon dioxide levels and fuel dependency with different configurations. In all electric propulsion systems, batteries are the only source of propulsive power on the aircraft [3]. In hybrid electric propulsion technology, propulsion energy is provided from an ideal combination of a conventional gas turbine engine (or internal combustion engine) and a kind of rechargeable energy storage system and at least one of them can supply electrical energy [4–8]. Turboelectric propulsion technology is defined as the batteryless form of hybrid electric propulsion system. Technological obstacles like inadequate battery energy densities; extreme weight problems originating from the number of batteries used; community acceptance issues (reliability and certification issues) on the novel system components manage the future of battery based propulsion technologies and it is estimated it has time to be developed and serviced [2, 9, 10]. Considering this shortcoming, turboelectric propulsion technology is seen as one step ahead.

Turboelectric propulsion systems do not include batteries. Thus, batteries are not a part of propulsion system for any phase of flight. Instead, gas turbine is

used to drive electric generator (alternator) directly and the electrical output is an input for power management system (inverters, converters, individual electric motors, distributed electric fans and so on) [11]. Turboelectric propulsion system structure is illustrated in Figure 1.

According to literature researches, generally, new generation propulsion system models are constructed on unmanned aerial vehicles (UAVs). Harmon [6] applies a cerebbellar model arithmetic computer (CMAC) neural network to control a paralel hybrid electric propulsion system of a small UAV. Hung and Gonzalez [12] overviews present and current developments and also the analysis of hybrid electric propulsion systems for small fixed-wing UAVs in their study. A hybrid electric light aircraft model is formed by Frosina et al. [13]. Sliwinski et al. [1] integrates hybrid electric propulsion to an unmanned aircraft.

In this paper, simulation of a high fidelity turboshaft engine-alternator model for turboelectric propulsion system is derived. To develop an aero-thermal engine model, GE T700 turboshaft engine data is used and constructed model is connected to an alternator model on MATLAB/Simulink environment. It is expected that this paper will make a contribution to new generation propulsion system research and design studies generally. Specifically, turboelectric propulsion system design and series hybrid electric propulsion system design studies will be able to be conducted easily and properly by using this type of mathematical models. Because, the proposed model can be easily extended to power system design and power management studies. Next section gives brief information about the turboshaft engine steady-state aero-thermal model and the alternator model. In section three, simulation results are presented and evaluated. Future works are specified as a conclusion in section four.

Turboshaft engine aero-thermal model

In this study, GE T700 turboshaft engine is preferred to model a high-fidelity aero-thermal model of the gas turbine engine in the turboelectric propulsion system. It is composed of 5-stage axial and a single-stage radial compressor. On the axial compressor, the first two stages have variable-geometry inlet guide vanes and stator vanes. Both gas generator turbine (HPT) and power turbine (PT) are formed of two stages. There is a turbine blade cooling mechanism at the HPT. The turboshaft includes a free PT. To model transient dynamics of turboshaft engine and thermodynamic processes inside; real component map data, some differential and non-algebraic equations are used. Engine parameters like temperature, pressure, mass flow, rotational speed are calculated per component. Bleed flows, HPT turbine cooling and mass flow during transient dynamics are also considered in the developed model. Parameters and formulas to develop the aero-thermal model of the engine are taken from [14–16]. A cross-sectional view of GE T700 is shown in Figure 2. Some design point values of GE T700 turboshaft engine and related input parameters for the simulation model are presented in Table 1 [14, 15].

Parts of the engine are evaluated separately and then they are entegrated to form GE T700 Turboshaft Engine aero-thermal model. Output condition at one component is assumed as an input condition of the next one. The flowchart of the aerothermal model is presented in Figure 3.

Modelling of inlet

At the compressor inlet, total temperature and pressure values are assumed to be equal to the ambient

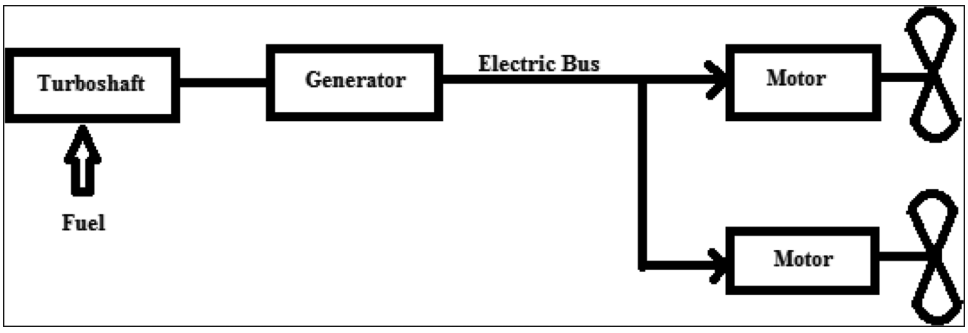

Figure 1: Turboelectric propulsion system structure.

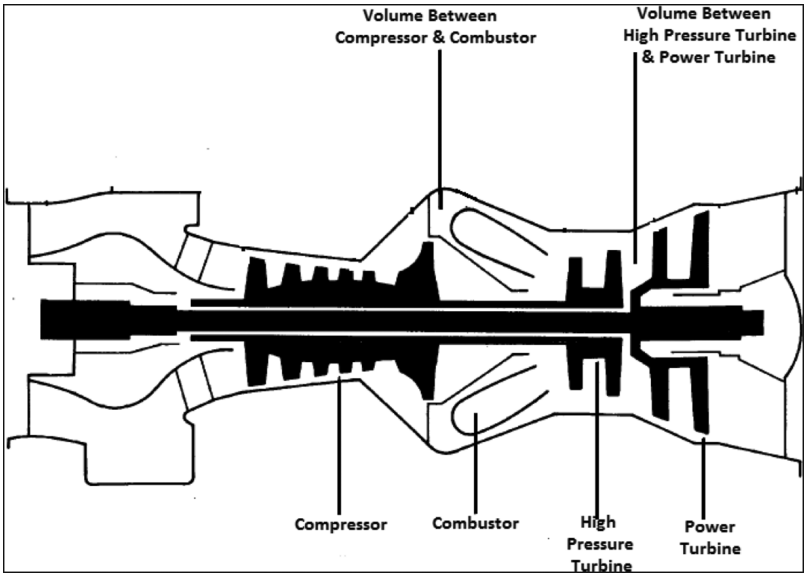

Figure 2: Cross-sectional view of GE T700 turboshaft engine.

Table 1: Some Initial Parameters and Design Point Values for the T700 Turboshaft Engine Aero-thermal Model.

Parameter	Value
R	287 J/kgK
LHV	42,565,836 J/kg
T_{atm}	288.15 K
P_{atm}	101,325 Pa
N_1	44,700 rev/min
N_2	20,900 rev/min
J_{HPT}	0.06033 Nms^2
J_{PT}	1.3694 Nms^2
V	0.004 m^3
σ	0.97
η_b	0.985
π_{comp}	17.53
τ	0.01 s

conditions as expressed in eqs. (1–2). Using MATLAB/Simulink International Standard Atmosphere (ISA) model [17], altitude variations are considered.

$$P_1 = P_{amb} \tag{1}$$

$$T_1 = T_{amb} \tag{2}$$

Modelling of compressor

Mass flow rate variations through the compressor component is developed with an ANFIS model. The ANFIS model uses a corrected compresor-HPT rotational shaft speed and compressor pressure ratio values as inputs and gives the compressor corrected mass flow rate as an output by means of the compressor performance map given by Ballin [14]. Detailed information about ANFIS can be found in [18]. Corrected compressor mass flow rate prediction results via ANFIS structure with training data is presented in Figure 4.

Corrected mass flow rate in compressor component can be described as follows:

$$\dot{m}_{2pcorr} = f\left(\pi_{comp}, N_{1corr}\right) \tag{3}$$

Mass flow rate at the compressor outlet is calculated by:

$$\dot{m}_{2p} = \dot{m}_{2pcorr} \times \frac{\delta}{\sqrt{\theta}} \tag{4}$$

Four various bleed flows are seen within the T700 turboshaft engine. These are:

- Two of them from the 4th compressor stage,
- Two of them from the diffuser.

These bleed flows are expressed as functions of the corrected compressor-HPT rotational shaft speed and the corrected mass flow rate with parameters b_1, b_2, b_3 in [14]. In the simulation model, suitable lookup tables developed in MATLAB/Simulink are used to define bleed flow proportions [17]. Bleed flow rate is described by eq. (5). Mass flow rate at the inlet of the first volume, before combustion chamber, is formulated as the difference between compressor output mass flow rate and bleed flow rate as seen in eq. (6).

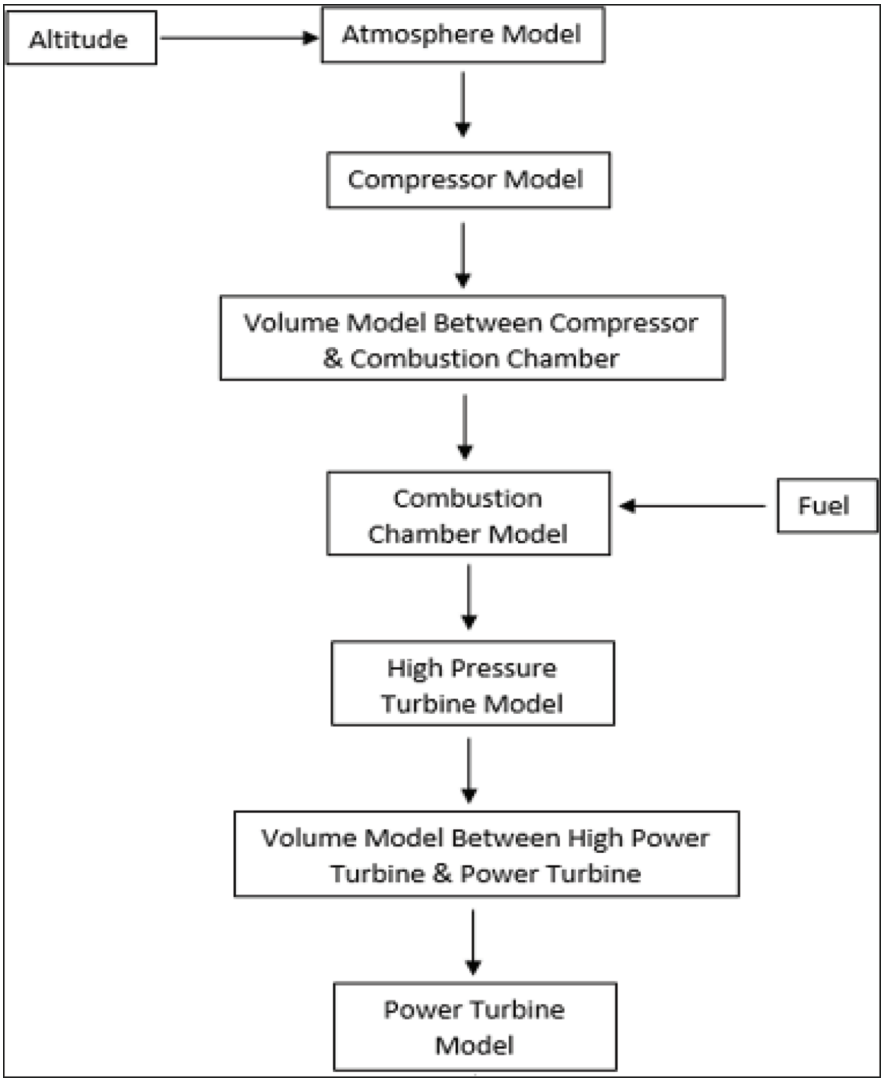

Figure 3: The flowchart of the aerothermal model.

$$m_{bleed} = \dot{m}_{2p} \times (b_1 + b_2 + b_3 + 0.0025) \quad (5)$$

$$\dot{m}_2 = \dot{m}_{2p} - \dot{m}_{bleed} \quad (6)$$

Generally, compressor output temperature is calculated with a formula that includes compressor efficiency (from performance map), pressure ratio and specific heat ratio variables. Ballin [14], evaluates the variation of compressor output temperature with a function of the compressor pressure ratio. Thus, temperature value at the compressor outlet is defined by eq. (7).

$$T_2 = T_1 \times f(\pi_{comp}) \quad (7)$$

Power absorbed by the compressor component is calculated by the following equation in [14]:

$$P_{comp} = \dot{m}_{2p} \times (h_2 - h_1) - 0.29 \times \dot{m}_{2p} \times h_2 \times (b_1 + b_2) \quad (8)$$

Modelling of combustion chamber

In modelling combustion chamber, it is assumed as an unsteady energy accumulator [14–16, 19]. Kinetic energy, time variation of mass and specific heat capacity of the flow inside combustion chamber are neglected because of low speed kinetic energy and time rate of change of combustion chamber temperature. Temperature and pressure values are assumed to be homogeneous and equal to the outlet conditions. They are also assumed as HPT inlet conditions. Combustion chamber outlet temperature value is calculated by eq. (9):

Figure 4: Compressor Mass Flow Rate Prediction Results via ANFIS with Training Data.

$$\frac{dT_3}{dt} = \frac{\dot{m}_2 \times h_2 + \dot{m}_f \times \eta_b \times LHV - \dot{m}_3 \times h_3}{\tau \times \dot{m}_3 \times C_{p_{gas}}} \tag{9}$$

Total pressure value at the combustion chamber outlet is expressed as a function of compressor inlet pressure by a pressure drop coefficient. It may be expressed as:

$$P_3 = P_2 \times \sigma \tag{10}$$

Modelling of HPT and PT

HPT outlet temperature value and entalpy values in compressor and combustion chamber are obtained using emprical entalpy-temperature relations to construct a high fidelity turboshaft model as in [14]. Besides, entalpy and mass flow rate values in HPT, power extracted by PT and PT outlet pressure values are read from data maps from Ballin [14] and they are used with suitable curve fitting techniques and MATLAB/Simulink lookup tables to model turbine characteristics. Power delivered by the HPT is calculated using eq. (11):

$$P_{HPT} = \dot{m}_{4p} \times \left(h_3 - h_{4p}\right) \tag{11}$$

Modelling of unsteady mass balance

During transient operating conditions, to solve mass imbalance problem inside engine components, two inter-component volumes are defined between compressor–combustion chamber and HPT-PT [19, 20]. Thus, mass imbalance between components are projected on the inter-component volume's pressure values. By this way, the pressure dynamics inside defined capacities is calculated using eq. (12).

$$\frac{dP_{out}}{dt} = \frac{\Delta m \times \gamma \times R \times T_{out}}{V} \tag{12}$$

Modelling of shaft dynamics

HPT or PT shaft dynamics on acceleration and deceleration conditions that are caused by power imbalances during transient operations are defined via eqs. (13–14):

$$\frac{dN_1}{dt} = \frac{1}{J_{HPT} \times N_1}\left(P_{HPT} - P_{comp} - P_{HPTloss}\right) \tag{13}$$

$$\frac{dN_2}{dt} = \frac{1}{J_{PT} \times N_2}\left(P_{PT} - P_{LOAD} - P_{PTloss}\right) \tag{14}$$

Modelling of gas properties

Modelling of specific heat values belong to air and gas forms are done by means of temperature dependent polynomial functions. Considering the temperature value of air or gas form, its temperature interval is detected. Whether it is between 200–800 K or 800–2200 K, the suitable polynomial function is selected and specific heat value is calculated [21, 22].

Modelling of alternator

Generators are electrical machines that convert mechanical power into electrical power. Alternator is a common generator type that is used for creating alternative current (AC). Power type conversion process is observed through a magnetic field and its operation principle depends on elecromagnetic induction. They are driven by steam turbines, gas turbines, water turbines, internal combustion engines and so on. It includes two parts: rotating one called rotor and steady one called stator. Stator part is composed of armature windings which are connected 120 degrees apart (3-phase) from others either in delta form or star form connection to generate AC output. DC excited field windings are located on rotor part.

Rotor structures can be evaluated in two different categories. Cyclindrical rotor types are preferred for high speed applications. Salient pole rotor types are proposed for low and medium speed applications.

In this study, to model an alternator, a synchronous machine block from MATLAB/Simulink SimPowerSystems Toolbox is used. This block has two inputs as exciting voltage "V_f" and mechanical power "P_m". Besides, angular velocity "w" is another possible input instead of mechanical power. The sign of the mechanical power defines the operating mode of the machine (positive power for generator mode and negative power for motor mode). It has two rotor selections as cyclindrical rotor and and salient pole rotor. Three line to line voltage outputs "A", "B", "C" and a collective output "m" that includes other calculated signals can be easily evaluated and used for feasible power management system designs for new generation propulsion systems. Detailed theorical information and formulation about mechanical part and electrical part of the synchronous machine block can be found in [23, 24]. General view of this block is presented in Figure 5.

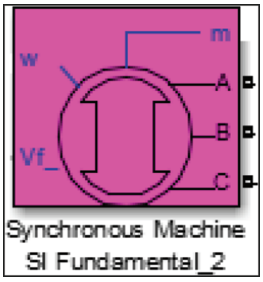

Figure 5: MATLAB/Simulink SimPowerSystems Toolbox synchronous machine Block.

Simulation results

The model developed in this paper is verified in a MATLAB/Simulink environment over a time frame of 20 seconds with a sampling time 0.0001. During simulations, the aero-thermal model of GE T700 turboshaft engine is run at design point to achieve maximum efficiency without any control mechanism and at steady state condition, power interchange relations between compressor-HPT and PT-alternator components are defined with the following eqs. (15–16). The aero-thermal model simulation results are compared to engine design point data used by [14–16] and presented in Figures 6–11.

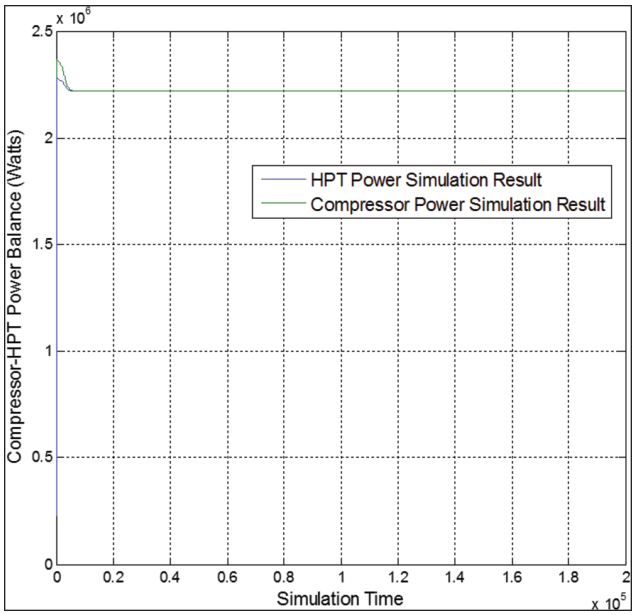

Figure 6: Compressor-HPT Steady-State Power Matching.

$$P_{comp} = P_{HPT} \tag{15}$$

$$P_{gen} = P_{PT} \tag{16}$$

Compressor-HPT steady-state power matching is evaluated at design point and simulation result is illustrated in Figure 6. Simulation result show that there is satisfactory overlapping between power dissipated from compressor and power generated by HPT considering error value.

Pressure values in terms of components are shown in Figures 7–8. It is clear that Simulink model results are higher than the engine design point data in all simulations. The errors percentages are found as 2.6 %, 0.86 % and 0.38 % for combustion chamber inlet - outlet and power turbine inlet pressures respectively.

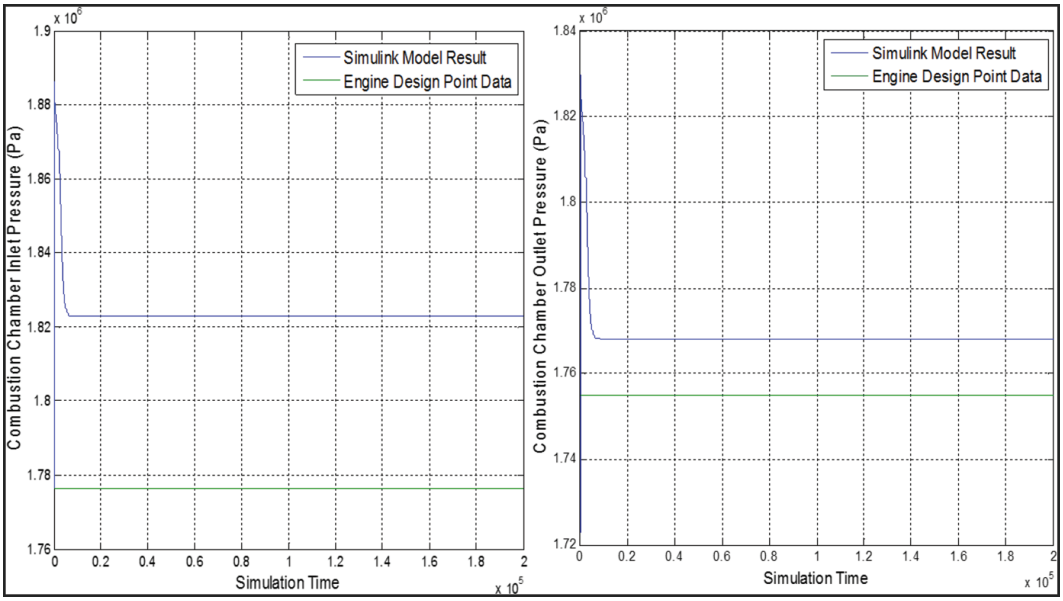

Figure 7: Combustion Chamber Inlet and Outlet Pressure Simulation Results.

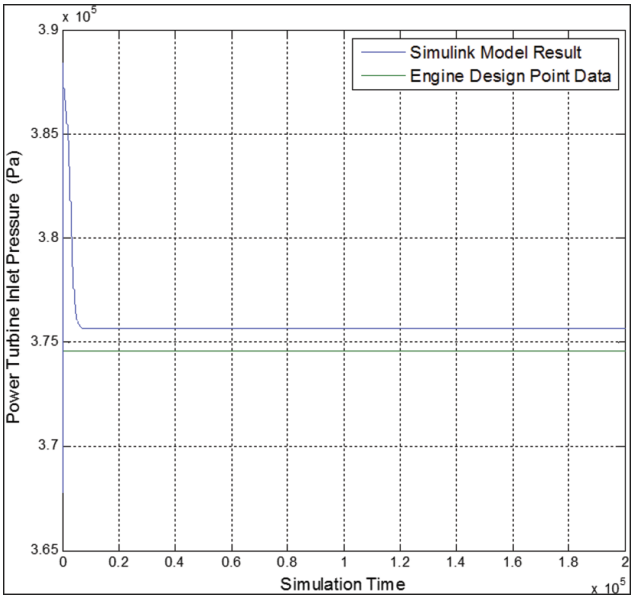

Figure 8: Power Turbine Inlet Pressure Simulation Results.

Simulink model calculates higher temperature values for compressor outlet and power turbine inlet however, lower temperature value is observed for combustion chamber outlet. In Figures 9–10, simulation results of the temperature values are exhibited. Considering related figures, the error percentages are calculated as 1.9 % for compressor outlet, 0.75 % for combustion chamber outlet and 3.8 % for power turbine inlet respectively.

Figure 11 illustrates the individual rotational shaft speed simulation results belong to compressor-HPT and PT-alternator. Simulink results are found to be lower than engine design point values in simulations. The error percentage of compressor-HPT rotational shaft speed is found as 1.83 % and the deviation of power turbine-alternator rotational speed is calculated as 0.28 %.

The alternator model used in the simulations is a 555 MVA, 24 kV, 60 Hz and 3600 rpm synchronous generator [23]. It includes a cyclindrical type rotor. A gearbox reduction mechanism is used with a proportion of "5.806" to match power turbine angular speed and rotor angular speed of the alternator (20,900 rev/min to 3600 rev/min). Exciting voltage V_f is defined as 10.9 V and i_{fn} is assumed as 0 A. The synchronous generator is operated under no load condition (load = 0. 1 % of nominal power). Detailed information about used synchronous machine design and block parameters can be found from [23, 24].

Power of PT, electrical power and rotor angular speed simulation results are presented in Figures 12–13 respectively. Power of PT is calculated higher than engine design point data however, rotor angular speed is lower than design point data in simulations. The error percentages that are belong to power of PT and rotor angular speed are calculated as 0.48 % and 0.29 % respectively. Steady-state power matching between PT mechanical power and alternator electrical power gives satisfactory overlapping considering error value in Figure 12. Summary of the deviations in terms of error percentages per engine parameters is

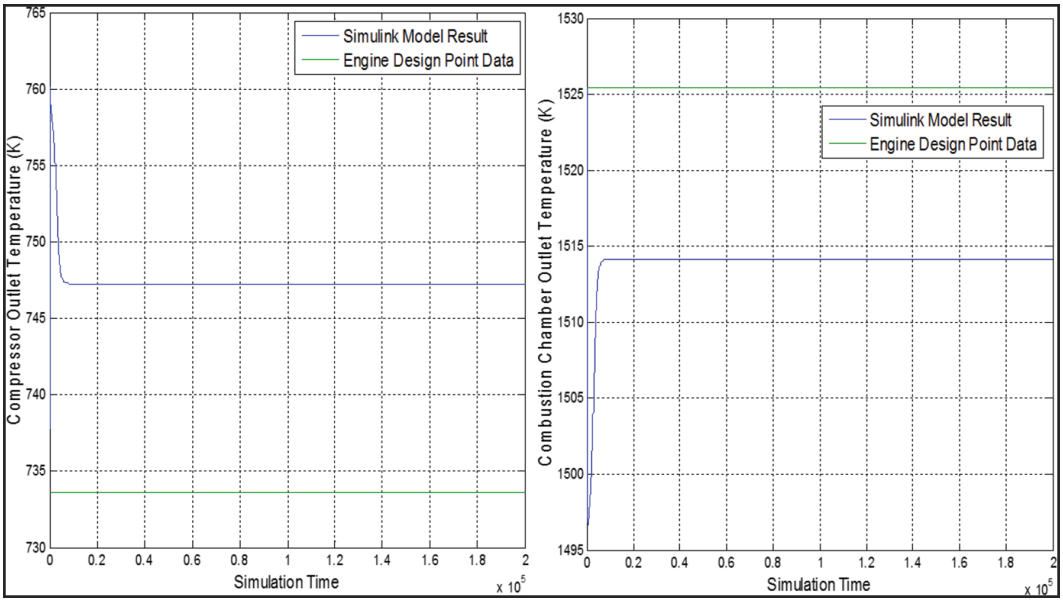

Figure 9: Compressor and Combustion Chamber Outlet Temperature Simulation Results.

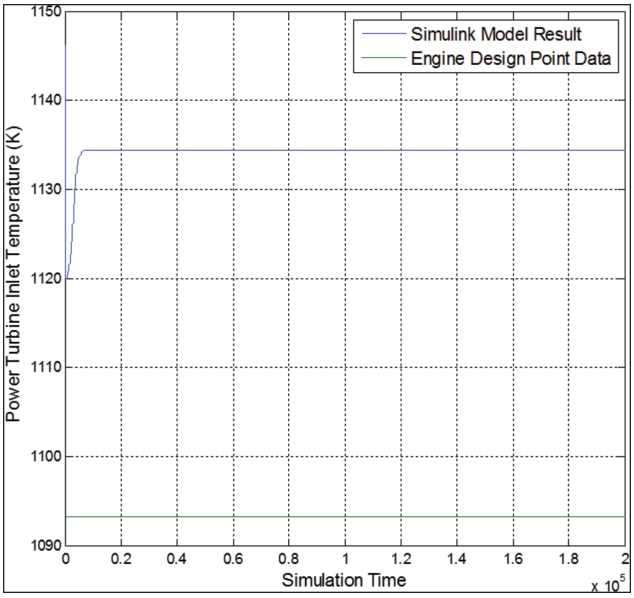

Figure 10: Power Turbine Inlet Temperature Simulation Results.

presented in Table 2. As a general view, they are acceptable. In simulations, calculation of some engine parameters (bleed air flow, compressor mass flow rate and so on) are required to use interpolation techniques. To reduce deviations per engine parameters and to enhance simulation results, other various interpolation techniques may be preferred or number of data that is needed for interpolation may be increased.

Conclusion

In this paper, simulation of a high fidelity turboshaft engine-alternator model for turboelectric propulsion system is derived. To develop an aero-thermal engine model, a GE T700 turboshaft engine data is used and its dynamic model is connected to an alternator model on MATLAB/Simulink environment. Open-loop simulations are performed and satisfactory results are obtained. It is expected that the proposed model can be easily extended to power system design and power management studies of turboelectric propulsion systems. This paper will also make a contribution to other new generation propulsion system research and design studies. Turboelectric propulsion system design and series hybrid electric propulsion system design studies can be conducted easily and properly by using this type of mathematical models. In the upcoming work, it is planning to integrate the current model with suitable converter, inverter, transformer, electric motor and/or energy storage system models to form a complete hybrid electric and/or turboelectric propulsion system structures for comparing and observing the differences in terms of conventional thrust, fuel savings and other performance parameters.

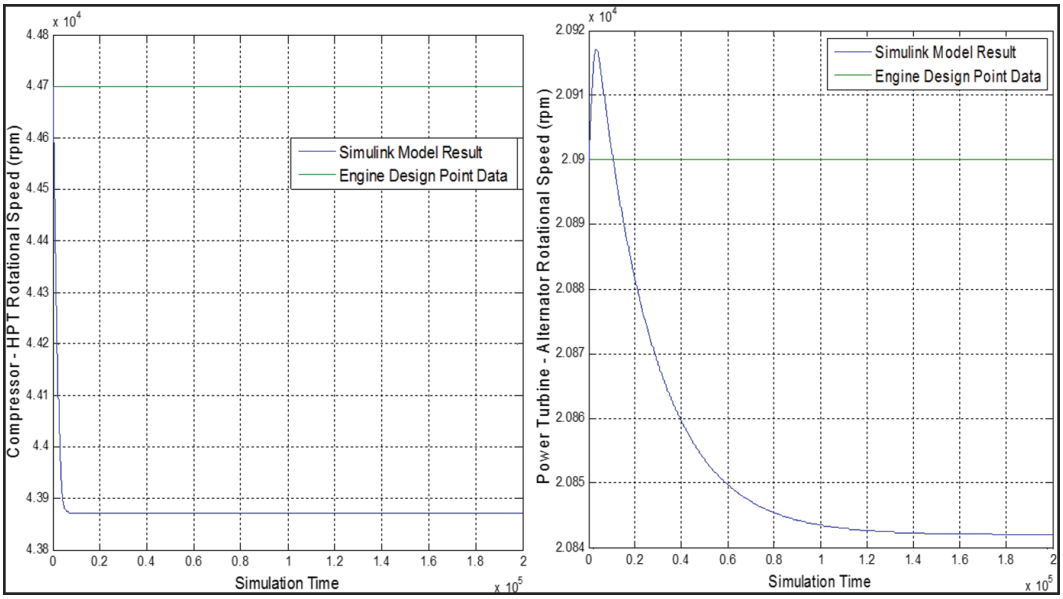

Figure 11: Compressor-HPT Rotational Speed and Power Turbine-Alternator Rotational Speed Simulation Results.

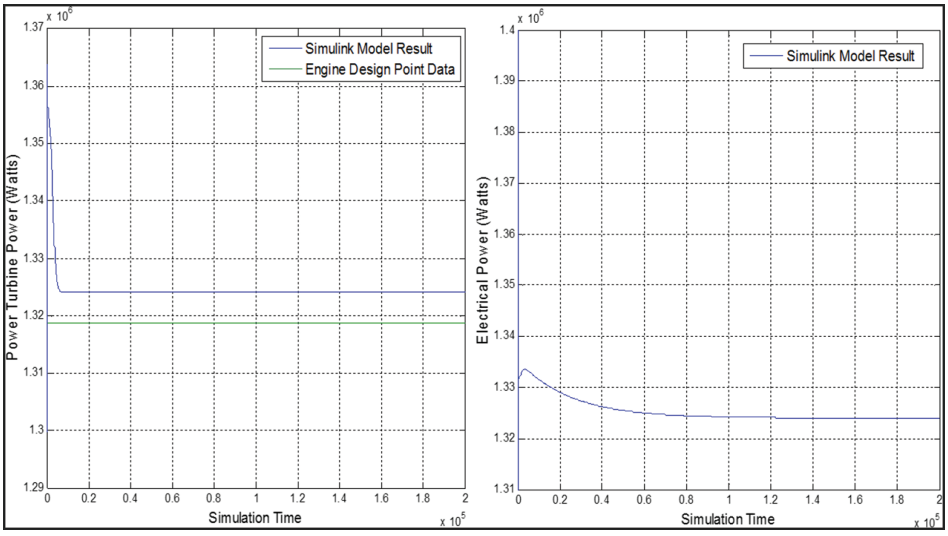

Figure 12: Power Turbine Power and Alternator Electrical Power Simulation Results.

Table 2: Deviation Percentages of the Mathematical Model.

	Engine Design Point Data	Simulink Model Result	Error Percentage %
Combustion Chamber Inlet Pressure	1,776,227.25	1,823,000	2.6
Combustion Chamber Outlet Pressure	1,754,912.523	1,770,000	0.86
Power Turbine Inlet Pressure	374,586.078	376,000	0.38
Compressor Outlet Temperature	733.5579	747.5	1.9
Combustion Chamber Outlet Temperature	1525.4583	1514	0.75
Power Turbine Inlet Temperature	1093.2524	1135	3.8
Compressor-HPT Rotational Speed	44,700	43,880	1.83
Power Turbine-Alternator Rotational Speed	20,900	20,842	0.28
Power Turbine Power	1,318,708	1,325,000	0.48
Rotor Angular Speed	377	375.9	0.29

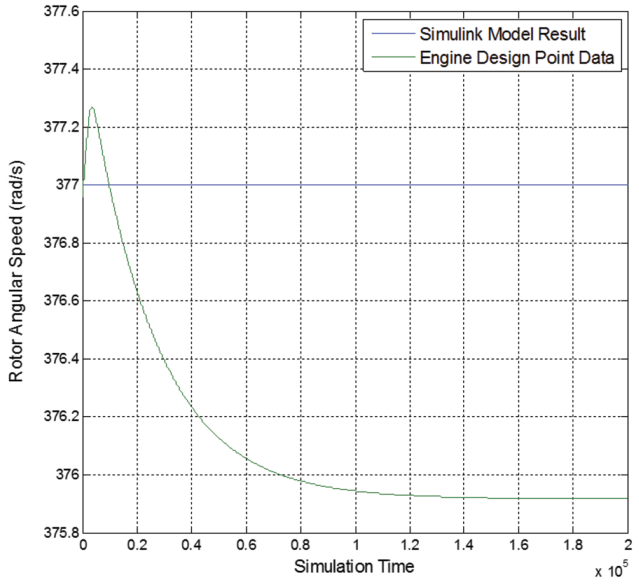

Figure 13: Rotor Angular Speed Simulation Results.

Nomenclature

ANFIS	Adaptive Neuro-Fuzzy Inference System
b_1, b_2, b_3	Bleed flow fractions
$C_{p,gas}$	Specific heat value of gas, J/kgK
f	Generic function
h_1	Entalpy value at the compressor inlet, J/kg
h_2	Enthalpy value at the compressor outlet, J/kg
h_3	Enthalpy value at the combustion chamber, J/kg
h_{4p}	Enthalpy value at the HPT outlet, J/kg
HPT	High-power turbine (gas generator turbine)
J_{HPT}	HPT moment of inertia
J_{PT}	PT moment of inertia
LHV	Lower heating value
$\dot{m}_{2p}$	Mass flow rate at the compressor outlet, kg/s
$\dot{m}_{2pcorr}$	Corrected mass flow rate inside the compressor, kg/s
$\dot{m}_2$	Mass flow rate at the first volume, kg/s
$\dot{m}_3$	Mass flow rate at combustion chamber, kg/s
$\dot{m}_{4p}$	Mass flow rate at HPT, kg/s
$\dot{m}_{bleed}$	Bleed air mass flow rate, kg/s
$\dot{m}_f$	Fuel flow rate, kg/s
Δm	Mass flow rate difference between the input and output of the component, J/kg
N_1	Compressor-HPT shaft rotational speed, rpm
N_{1corr}	Corrected compressor-HPT shaft rotational speed
N_2	PT shaft rotational speed, rpm
PT	Power turbine
P_{amb}	Ambient pressure, Pa
P_{comp}	Compressor power, Watts
P_{gen}	Generator power, Watts
P_{HPT}	HPT power, Watts
$P_{HPTloss}$	HPT power loss, Watts
P_{LOAD}	Load applied on the power turbine, Watts
P_{PT}	PT power, Watts
P_{PTloss}	PT power loss, Watts
P_{out}	Component output pressure, Pa
P_1	Compressor input pressure, Pa
P_2	Combustion chamber input pressure, Pa
P_3	Combustion chamber output pressure, Pa
T_{amb}	Ambient temperature, K
T_{out}	Component output temperature, K
T_1	Compressor input temperature, K
T_2	Compressor output temperature, K
T_3	Combustion chamber temperature, K
R	Gas constant
V	Volume
σ	Combustion chamber pressure loss coefficient
γ	Specific heat ratio
δ	Non-dimensional pressure, $\frac{P_{amb}}{P_{atm}} Pa$
θ	Non-dimensional temperature, $\frac{T_{amb}}{T_{atm}}$ K
τ	Combustion chamber time constant
π_{comp}	Compressor pressure ratio
η_b	Combustor efficiency

References

1. Sliwinski J, Gardi A, Marino M, Sabatini R. Hybrid-electric propulsion integration in unmanned aircraft. Energy. 2017;140:1407–16.
2. Riboldi CE, Gualdoni F, Trainelli L. Preliminary weight sizing of light pure-electric and hybrid-electric aircraft. Transp Res Procedia. 2018;29:376–89.
3. Ma S, Wang S, Zhang C, Zhang S. A method to improve the efficiency of an electric aircraft propulsion system. Energy. 2017;140:436–43.
4. Chan CC, Chau KT. Modern electric vehicle technology. Oxford New York: Oxford University Press, 2001.
5. Pornet C, Isikveren AT. Conceptualdesignofhybrid-electrictransportaircraft. Prog Aerospace Sci. 2015;79:114–13.
6. Harmon FG, Frank AA, Joshi SS, Application of a CMAC neural network to the control of a parallel hybrid-electric propulsion system for a small unmanned aerial vehicle. Proceedings of International Joint Conference on Neural Networks. Montreal, Canada. July 31 – August 4, 2005.
7. Tan YK, Mao JC, Tseng KJ. Modelling of battery temperature effect on electrical characteristics of li-ion battery in hybrid electric vehicle. IEEE PEDS. Singapore, 5–8 December 2011.
8. Thanagasundram S, Arunachala R, Makinejad K, Teutsch T. A cell level model for battery simulation. European Electric Vehicle Congress. Brussels, Belgium, 20–22 November 2012.
9. Ozawa K. Lithium-ion rechargeable batteries. WILEY-VCH Verlag GmbH & Co. KGaA, Weinheim, Germany, 2009.
10. Cao J, Peng J, He H. Modeling and simulation research on power-split hybrid electric vehicle. Energy Procedia. 2016;104:354–59.
11. National Academies of Sciences, Engineering, and Medicine. Commercial aircraft propulsion and energy systems research: reducing global carbon emissions. Washington, DC: The National Academies Press, 2016. Accessed: 31 September 2018. DOI:10.17226/23490.

12. Hung JY, Gonzalez LF. On parallel hybrid-electric propulsion system for unmanned aerial vehicles. Prog Aerospace Sci. 2012;51:1–17.
13. Frosina E, Caputo C, Marinaro G, Senatore A, Pascarella C, Di Lorenzo G. Modelling of a hybrid-electric light aircraft. Energy Procedia. 2017;126:1155–62.
14. Ballin MG, A high-fidelity real-time simulation of a small turboshaft engine. NASA-TM-100991, 1988.
15. Uzol O. A new high fidelity transient aerothermal model for real-time simulations of the t700 helicopterturboshaft engine. J Thermal Sci Technol. 2011;31:37–44.
16. Novikov Y. Development of a high-fidelity transient aerothermal model for a helicopter turboshaft engine for inlet distortion and engine deterioration simulations. Master of Science Thesis in Aerospace Engineering, Middle East Technical University. Turkey, 2012.
17. https://www.mathworks.com.
18. Jang JR. ANFIS: adaptive-network-based fuzzy inference system. IEEE T Syst Man Cyc. 1993;23:665–85.
19. Camporeale SM, Fortunato B, Mastrovito M. A modular code for real-time dynamic simulation of gas turbines in simulink. ASME J Eng Gas Turbines Power. 2006;128:506–17.
20. Gaudet SR. Development of a dynamic modeling and control system design methodology for gas turbines. Master of Applied Science Thesis. Department of Mechanical and Aerospace Engineering, Carleton University, Ottawa, Ontario, Canada. 2007.
21. Chappel MS, Cockshutt EP. Gas turbine cycle calculations: thermodynamic data tables for air and combustion products for three systems of units. NRC No:14300. Ottowa, Canada, 1974.
22. Al-Hamdan QZ, Ebaid MSY. Modeling and simulation of a gas turbine engine for power generation. J Eng Gas Turbines Power. 2006;128:302–11.
23. https://www.mathworks.com/help/physmod/sps/powersys/ref/synchronousmachine.html.
24. Kundur P. Power system stability and control. McGraw-Hill, USA, 1994.